Metal–Organic Frameworks Hot Paper

How to cite: *Angew. Chem. Int. Ed.* **2021**, *60*, 14124–14130
International Edition: doi.org/10.1002/anie.202104366
German Edition: doi.org/10.1002/ange.202104366

Large-Area Crystalline Zeolitic Imidazolate Framework Thin Films

Zhi Chen, Rui Wang, Tao Ma, Jin-Long Wang, Yu Duan, Zhi-Zhan Dai, Jie Xu, Hui-Juan Wang, Jiayin Yuan, Hai-Long Jiang, Yue-Wei Yin, Xiao-Guang Li, Min-Rui Gao, and Shu-Hong Yu**

Abstract: *We report that continuous MOF films with highly controlled thickness (from 44 to 5100 nm) can be deposited over length scales greater than 80 centimeters by a facile, fast, and cost-effective spray-coating method. Such success relies on our discovery of unprecedented perfectly dispersed colloidal solutions consisting of amorphous MOF nanoparticles, which we adopted as precursors that readily converted to the crystalline films upon low-temperature in situ heating. The colloidal solutions allow for the fabrication of compact and uniform MOF films on a great deal of substrates such as fluorine-doped tin oxide, glass, SiO_2, Al_2O_3, Si, Cu, and even flexible polycarbonate, widening their technological applications where substrates are essential. Despite the present work focuses on the fabrication of uniform cobalt-(2-methylimidazole)$_2$ and zinc-(2-methylimidazole)$_2$ films, our findings mark a great possibility in producing other high-quality MOF thin films on a large scale.*

Introduction

Metal–organic frameworks (MOFs) are an important class of crystalline materials with tunable porosity,[1] topology[2] and functionality,[3] which have been specifically designed for a wide range of applications such as molecular separation,[4] gas storage,[5] sensors,[6] microelectrics[7] and catalysis.[8] These application areas commonly built on the availability of continuous MOF thin films adopted in related nanotechnological devices. However, the fabrication of MOF films faces significant scientific and technical challenges because processing these crystalline coordination polymers into films often lead to structural inhomogeneities such as wrinkles, cracks and apparent porosity, which would strongly affect the film performances.

Since the seminal work from Fischer and co-workers who prepared MOF-5 film on an Au (111) substrate in 2005,[9] intense research efforts have been made to establish robust synthesis methods for producing high-quality MOF films. Thus far, several strategies that enable the fabrication of well-defined MOF films have been developed, including hybrid mixed-matrix approach,[10] solvothermal synthesis,[11] layer-by-layer method[7d] and electrodeposition.[12] Other fabrication methods that yield MOF films for specific requirements have also been proposed. Falcaro and co-workers reported the heteroepitaxial growth of polycrystalline MOF film on a copper hydroxide substrate, where the obtained centimeter-scale MOF film is precisely aligned.[13] Ameloot et al. described a chemical vapour deposition (CVD) process for making uniform and conformal ZIF-8 film on high-aspect-ratio features.[14] Bein et al. developed a vapor-assistant conversion (VAC) method to obtain highly oriented zirconium-based MOF thin films.[15] Although remarkable success has been achieved, these methods also impose certain limitations. For example, solvothermal synthesis raises processability and safety concerns, electrodeposition requires (semi)conducting substrates, heteroepitaxial growth requires specific substrate that directs the growth of MOF crystals, and CVD process usually constrains to ultrahigh vacuum. Furthermore, no scalable processing method exists at present that could produce large-area, uniformly high-quality MOF thin-films with thickness smaller than 44 nm.

[*] Dr. Z. Chen, Dr. R. Wang, Dr. J. L. Wang, Dr. Y. Duan, Prof. H. L. Jiang, Prof. M. R. Gao, Prof. S. H. Yu
Division of Nanomaterials & Chemistry, Hefei National Laboratory for Physical Sciences at the Microscale, Institute of Energy, Hefei Comprehensive National Science Center, CAS Center for Excellence in Nanoscience, Institute of Biomimetic Materials & Chemistry, Anhui Engineering Laboratory of Biomimetic Materials, Department of Chemistry
University of Science and Technology of China
Hefei 230026 (China)
E-mail: mgao@ustc.edu.cn
shyu@ustc.edu.cn

Dr. T. Ma
Shenzhen Key Laboratory for Functional Polymer, College of Chemistry and Environment Engineering, Shenzhen University
Shenzhen, Guangdong 518060 (China)

Dr. Z. Z. Dai, Prof. Y. W. Yin, Prof. X. G. Li
Hefei National Laboratory for Physical Sciences at the Microscale, Department of Physics, and
CAS Key Laboratory of Strongly-coupled Quantum Matter Physics
University of Science and Technology of China
Hefei 230026 (China)

J. Xu
Institute of Functional Nano and Soft Materials (FUNSOM) & Collaborative Innovation Center of Suzhou Nano Science and Technology, Soochow University
Suzhou 215123 (China)

H. J. Wang
Experimental Center of Engineering and Material Science
University of Science and Technology of China
Hefei 230026 (China)

Dr. J. Yuan
Department of Materials and Environmental Chemistry
Stockholm University, 10691 Stockholm (Sweden)

Prof. X. G. Li
Collaborative Innovation Center of Advanced Microstructures
Nanjing, 210093 (China)

Supporting information and the ORCID identification number(s) for the author(s) of this article can be found under: https://doi.org/10.1002/anie.202104366.

Herein, we report on the discovery of an unconventional ZIF-67 (i.e., cobalt-(2-methylimidazole)$_2$,[5c] a zeolitic imidazolate framework (ZIF) subclass of MOFs) colloidal dispersion consisting of completely dispersed amorphous nanoparticles in methanol. Using such sticky colloidal solutions as precursors, we show that uniform films can be deposited onto a number of substrates (e.g., fluorine-doped SnO_2 (FTO), glass, SiO_2, Al_2O_3, Si, Cu, and even flexible polycarbonate) by a facile, fast, and cost-effective spray-coating approach at low temperatures in air, enabling fabrication of large-area ZIF-67 thin films (up to 4800 cm^2) with highly controlled thickness (from 44 to 5100 nm). The same fabrication methodology can be extended to produce other high-quality MOF films, such as ZIF-8 (zinc-(2-methylimidazole)$_2$) thin film. We anticipate that the previously unknown colloidal MOF precursor could open up efficient routes of fabricating high-quality MOF thin films through spray coating for various applications.

Results and Discussion

ZIFs are an important class of porous materials with zeolite-type tetrahedral topologies, which consist of metal nodes (such as cobalt and zinc) bridged by imidazole.[16] We produced unprecedented amorphous ZIF-67 nanoparticulate precursor by simply mixing cobalt(II) acetate tetrahydrate ($Co(CH_3COO)_2{\cdot}4H_2O$) and 2-methylimidazole (Hmim) in methanol at room temperature (Figure 1 A). The achieved ZIF-67 colloidal precursor is highly stable without crystallization after aging in lab environment even for even 55 days (Supporting Information, Figures S1 and S2). Replacing $Co(CH_3COO)_2{\cdot}4H_2O$ with $Co(NO_3)_2{\cdot}6H_2O$, however, leads to conventional high-crystalline ZIF-67 crystals that reported previously[17] (Figure 1 B; Supporting Information, Figure S3). It is known that ZIF-67 crystals are structurally analogous to zeolites, in which Hmim donates a proton and couples with Co^{II} nodes to form CoN_4 tetrahedra.[18] An network of linked CoN_4 tetrahedra with Co-Hmim-Co angle of about 145° gives rise to the crystalline ZIF-67 structure[19] (Figure 1 B). We hypothesize that, in the presence of CH_3COO^-, the copolymerization of Co^{II} with Hmim ligands

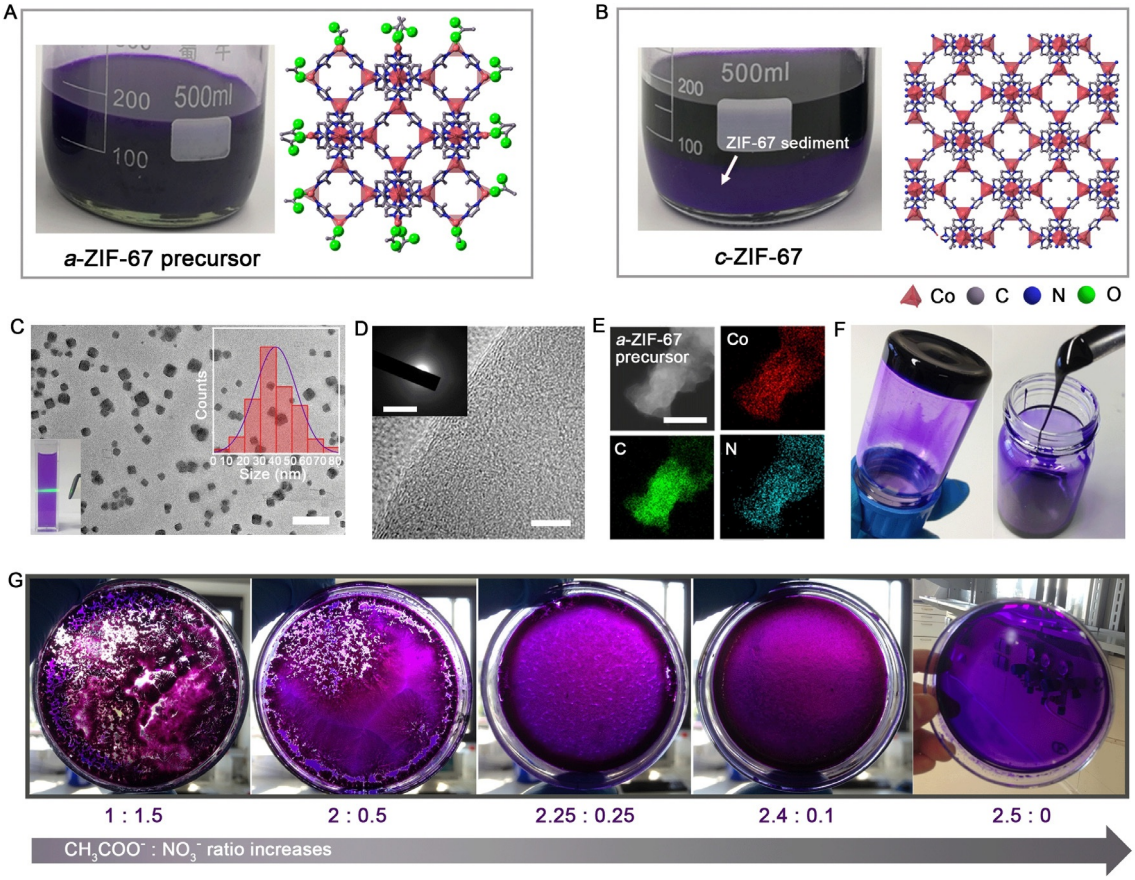

Figure 1. A),B) Photograph and the crystal structure of A) *a*-ZIF-67 precursor and B) *c*-ZIF-67. Co red, C gray, N blue, O green balls; H atoms are omitted for clarity. C) TEM image of *a*-ZIF-67 precursor nanoparticles. Scale bar: 200 nm. The upper inset shows the histogram of particle size in (C). The lower inset presents the Tyndall effect of the *a*-ZIF-67 colloidal solution. D) HRTEM of a typical *a*-ZIF-67 nanoparticle. Scale bar: 5 nm. Inset: corresponding SAED pattern obtained from the whole *a*-ZIF-67 precursor nanoparticle. Scale bar: 5 nm^{-1}. E) STEM image and corresponding elemental mappings of *a*-ZIF-67 precursor. Scale bar: 500 nm. (F) Photographs of the gel of *a*-ZIF-67 precursor. G) A photographic experiment series demonstrates the critical role of CH_3COO^- anions that limits the crystallization of ZIF-67, leading to the gelled *a*-ZIF-67 film.

would be partially blocked because of the relatively big anion size that brings steric hindrance by binding to Co (Figure 1 A). As a result, the nucleation of ordered linked CoN_4 tetrahedra is disrupted, leading to amorphous ZIF-67 precursor.

Representative transmission electron microscopy (TEM) image of the as-prepared ZIF-67 precursor in Figure 1 C reveals nanoparticles with an average size of about 40 nm (top inset in Figure 1 C). The colloidal dispersion of ZIF-67 precursor is in purple color, showing a Tyndall effect owing to light scattering by the nanoparticles in the colloidal dispersion (down inset in Figure 1 C). High-resolution TEM (HRTEM) and its corresponding selected-area electron diffraction (SAED) characterizations displays the absence of a crystalline phase (Figure 1 D and inset). Scanning TEM (STEM) elemental mapping reveals a uniform spatial distribution of Co, C, and N of the amorphous ZIF-67 (*a*-ZIF-67) precursor (Figure 1 E). Intriguingly, when methanol was evaporated naturally from the *a*-ZIF-67 colloidal precursor, a highly viscous gel can be formed (Figure 1 F; Supporting Information, Figure S4). Casting such sticky *a*-ZIF-67 precursor gel between two glass slides can bind them to an extend that withstands the weight of the glass slide (Supporting Information, Figure S5). We reason that the disordered and amorphous structure of *a*-ZIF-67 precursor gives rich dangling ligands with Hmim hydrogen bonding (N–H···N) chains,[20] which cause the marked adhesion. The *a*-ZIF-67 colloidal precursor with gel-like state of the concentrated species now enables the easy processing of pure ZIF films onto various substrates, which was thought to be a huge challenge before.

X-ray diffraction (XRD) patterns of our synthesized ZIF-67 precursor are given in the Supporting Information, Figure S6. The spectrum for the sample obtained using $Co(NO_3)_2{\cdot}6H_2O$ as precursor contains sharp XRD peaks that belong to crystalline ZIF-67 (*c*-ZIF-67)[17] (Figure 2 B), whereas the adoption of $Co(CH_3COO)_2{\cdot}4H_2O$ gives an amorphous product. Fourier transform infrared (FT-IR) spectroscopy analysis reveals that excess Hmim is retained on the surface of *a*-ZIF-67 precursor when not thoroughly washed[14,21] (Supporting Information, Figure S7). Moreover, Raman spectroscopy measurements exhibit one prominent peak at 195 cm^{-1} that corresponds to Co–N bond[22] (Supporting Information, Figure S8), revealing that Co^{II} coordinates with mim links as CoN_4 tetrahedra.

We then systematically optimized the synthetic parameters for achieving high-quality *c*-ZIF-67 films from the colloidal dispersions. Our control experiments reveal that the addition of some of the stoichiometrically missing $Co(NO_3)_2{\cdot}6H_2O$ in the recipe causes crystalline ZIF-67 precipitation that precludes the formation of a dense and continuous

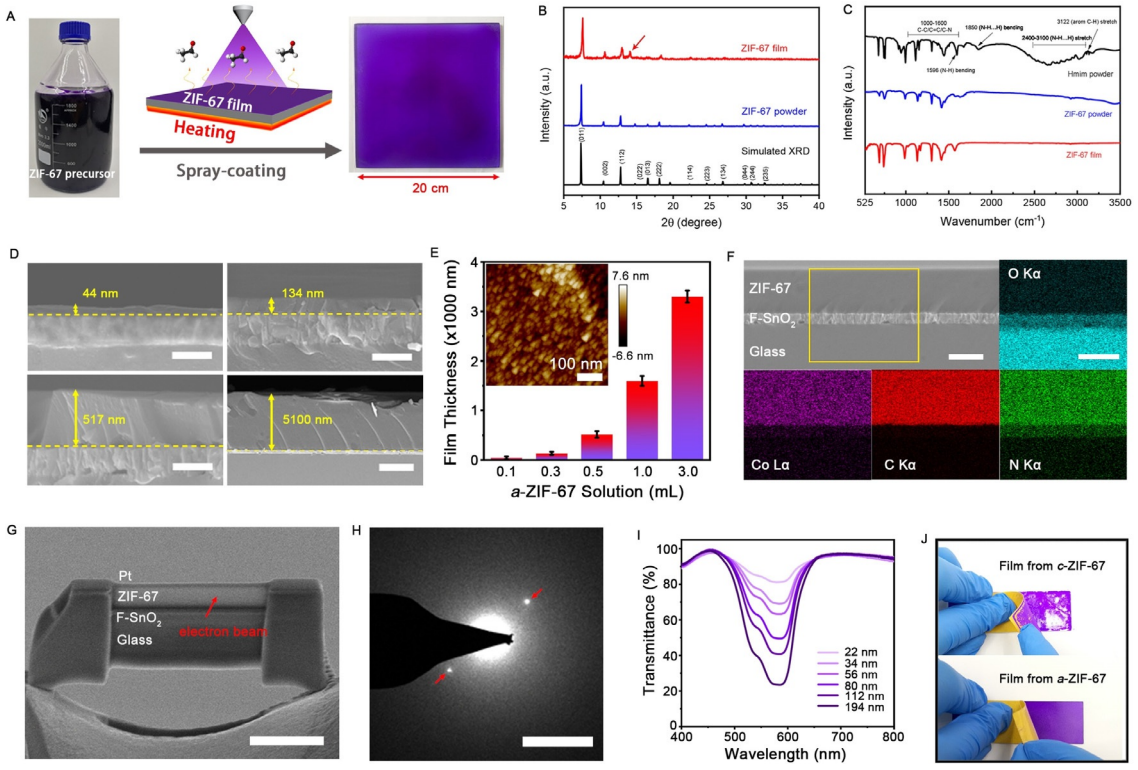

Figure 2. A) The spray-coating route to a 20 cm × 20 cm crystalline ZIF-67 film from *a*-ZIF-67 precursor. B) XRD patterns of ZIF-67 film and conventional ZIF-67 powder with a simulated XRD pattern for comparison. C) FTIR spectra of ZIF-67 powder, ZIF-67 film and pure Hmim. D) Cross-sectional SEM images of films with different thickness on FTO glass substrate. Scale bars: 400 nm, 400 nm, 400 nm, and 3 μm. E) Film thickness as a function of the dosage of *a*-ZIF-67 precursor dispersion. Typical AFM topography is shown as inset. F) SEM and EDS cross-sectional maps of a ZIF-67 film on FTO glass substrate. Scale bars: 500 nm. G) Focused ion beam (FIB) cross-sectional image of the ZIF-67 film, which was directly used for the low-dose SAED analysis. Scale bar: 2 μm. H) SAED pattern acquired at the ZIF-67 film marked by red arrow in (G), showing sharp diffraction spots. Scale bar: 2 nm^{-1}. I) Light transmittance of ZIF-67 films with different thickness. J) Photographs illustrate the striking robustness of ZIF-67 film obtained by spray-coating *a*-ZIF-67 precursor dispersion on FTO glass substrate.

film (Figure 1G; Supporting Information, Figures S4, S9, S10). The *a*-ZIF-67 colloidal precursor is ideally suited for the scalable fabrication of ZIF-67 films. As schematically shown in Figure 2A, the *a*-ZIF-67 colloidal precursor can be straightforwardly spray-coated onto a FTO glass substrate to yield film. In this process, we used a hot-casting route to heat the substrate up to 250 °C, which accelerates the methanol evaporation rate that avoids possible aggregation during the spray-coating process. The XRD pattern of the obtained film shows diffraction peaks identical to ZIF-67 powder synthesized by conventional route (Figure 2B), indicating that the amorphous ZIF-67 precursor was crystallized in situ on the FTO substrate, forming a crystalline ZIF-67 film (Supporting Information, Figures S11–S13). We note that the peak at 14.1° does not appear in the simulated pattern, which might attribute to certain unknown impurity in the film upon heating. Moreover, the FTIR spectrum of the obtained ZIF-67 film is also analogous to the ZIF-67 powder synthesized by conventional route (Figure 2C). As compared to pure Hmim, the N–H···H stretch between 2400–3100 cm^{-1} completely disappeared for our ZIF-67 film, suggesting that Hmim was deprotonated and incorporated into the ZIF-67 framework. No free Hmim molecules were detected.[14,21] We assume the excess methylimidazole liberated by the crystallization acts as a plasticizer and finally evaporates from the film. The hot-cast film looks compact and uniform, indicating formation of a high-quality ZIF film (20 cm × 20 cm; Figure 2A). Moreover, scaling up the film to even 0.6 m × 0.8 m was readily realized through this method using *a*-ZIF-67 as precursors (Supporting Information, Figure S14), which permits large-scale use of ZIF-67 films in diverse application areas.

Spray coating colloidal *a*-ZIF-67 precursor with in situ heating enables the thickness of deposited ZIF-67 films to be precisely controlled. Cross-sectional scanning electron microscopy (SEM) analyses show that compact films with thickness of 44, 134, 517, and 5100 nm were achieved (Figure 2D). The thickness of ZIF-67 films as a function of the dosage of *a*-ZIF-67 precursor are displayed in Figure 2E. Atomic force microscopy (AFM) measurement reveals that the as-obtained ZIF-67 film is very smooth (inset in Figure 2E), comparable to the smoothest MOF films reported thus far.[4d,14] It also uncovers that the film consists of small nanoparticles with an average size of about 33 nm, roughly agreeing with the particle size of 39.9 nm calculated by the Scherrer equation (Supporting Information, Figure S15). We note that the obtained ZIF-67 film is crack-free and offers continuous, uniform coverage of the FTO substrate with densely packed small particles (Supporting Information, Figure S11). Figure 2F gives a close-up cross-sectional SEM image and corresponding energy dispersive X-ray spectroscopy (EDS) mapping of the 660-nm-thick ZIF-67 film. A sharp interface between ZIF-67 film and FTO substrate is clearly observed, verifying that the film is perfectly confined to the substrate. Additionally, EDS mapping results illustrate the homogeneous composition of the deposited ZIF-67 film (Figure 2F). Cross-sectional TEM shows that ZIF film adheres on the FTO support very tightly (Figure 2G; Supporting Information, Figure S12). We acquired the selected area electron diffraction (SAED) pattern of the ZIF-67 film (red arrow in Figure 2G) on a low-dose TEM (5.79 e $nm^{-2} s^{-1}$), which shows sharp diffraction spots that correspond to the (112) spacing of the ZIF-67 phase (Figure 2H), evidencing its crystallinity.[23]

In Figure 2I we show the optical transmittance spectra of the ZIF-67 films with different thickness, which well follows the Beer–Lambert law (Supporting Information, Figure S16). On the transparent FTO substrate, a 22-nm-thick ZIF-67 film has an outstanding transmittance of 83% at 582 nm. This transmittance reduces to 23% when the film thickness reaches 194 nm (Figure 2I; Supporting Information, Figure S17). Furthermore, we compared the peel experiments on ZIF-67 films deposited by conventional ZIF-67 and our new colloidal *a*-ZIF-67 precursor. Figure 2J exhibits that conventional ZIF-67 film was cracked and separated from FTO substrate upon peeling, whereas there was no observable peel-off for the actual film. This difficult peel-off spotlights the importance of colloidal *a*-ZIF-67 with its functional stickiness and chemical surface termination for making robust film with strong adhesion to the substrates.

A challenging restriction inhibiting the advancement of MOF films is the universal deposition of films directly onto any desired substrates. With the unique and stable *a*-ZIF-67 precursor colloidal dispersion, large-area ZIF-67 thin films could be deposited onto a variety of substrates (2 cm × 2 cm) such as glass, SiO_2, Al_2O_3, Si, Cu, and even flexible polycarbonate (PC) by the spray coating method (Figure 3A; Supporting Information, Figures S18, S19). Intriguingly, the ZIF-67 film on PC substrate shows exceptional flexibility and robustness even when subjected to rigorous twisting (Figure 3B), whereas the film made from conventional ZIF-67 is highly brittle (Supporting Information, Figure S20). Cross-sectional SEM images reveal good adhesion of ZIF-67 films to these substrates although they possess different chemical and surface nature (Figure 3C–H; Supporting Information, Figures S18, S19). This indicates different adapted and self-organized binding layers. Moreover, the achieved ZIF-67 films on aforementioned substrates exhibit good homogeneity with only minor defects or bulges (Figure 3C–H; Supporting Information, Figures S18, S19). We emphasize that the formation of high-quality ZIF-67 films on these substrates (especially on flexible PC substrate) is remarkable, demonstrating that the new colloidal *a*-ZIF-67 offers an efficient route of making previously unachievable MOF thin films.

In recent years, MOFs have been developed as high-dielectric-constant (high-*k*) materials for high-electron-mobility transistors and thin-film transistors considering their readily designed and functionalized crystalline porous structures.[24] Despite zirconium dioxide and hafnium dioxide have previously been investigated as high-*k* dielectric materials, they are unfortunately too brittle to be compatible with substrates.[25] We thus reason that the robust ZIF-67 thin film on FTO enabled by spray-coating method opens a way to high-quality high-*k* dielectric material for advanced electronic devices.

We measured the high-*k* value of our ZIF-67 thin film, and the dielcctric constant of the conventional ZIF-67 powder (press to tablet) was also probed for comparison (Figure 4A;

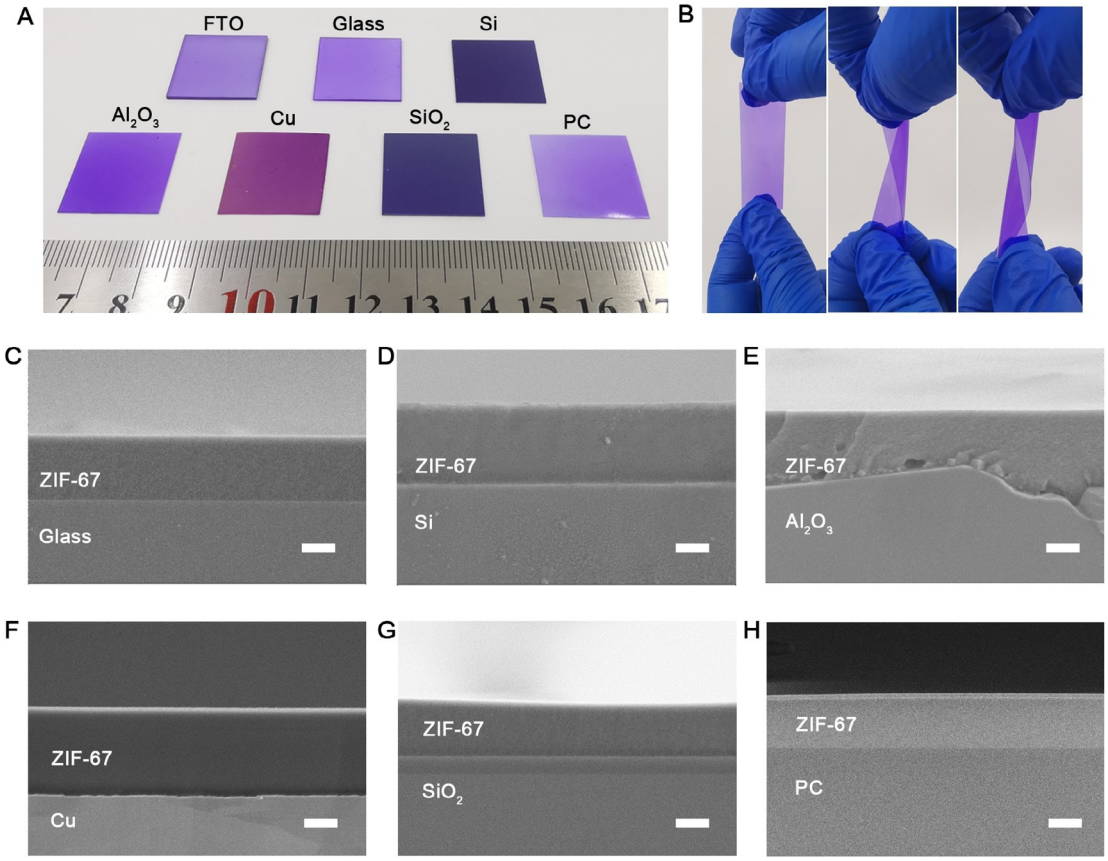

Figure 3. A) Photographs of ZIF-67 films deposited onto different substrates (FTO, glass, SiO_2, Al_2O_3, Si, Cu, and PC, respectively). B) Photographs of ZIF-67 films on PC in different twisting states. (C–H) SEM cross-sectional images of ZIF-67 films on Glass, Si, Al_2O_3, Cu, SiO_2 and PC. Scale bars: 500 nm.

Supporting Information, Figure S21). At room temperature, the ZIF-67 film shows a high-*k* value of 4.5 at 1 kHz, which is larger than that of 4.25 obtained on the ZIF-67 powder (Figure 4B). Moreover, a very small dissipation factor was observed on the ZIF-67 film. We highlight that the high-*k* value of the ZIF-67 film compares favorably to previously reported HKUST-1 with value of 1.7 and $[Zn_4O(CO_2)_6]$ with value of 1.33.[26] These results promise the development of robust MOF thin films with good dielectric properties for microelectronics.

Although the present work focuses on ZIF-67, we note that our approach can be extended to other MOFs, such as ZIF-8-another prototypical MOF material.[27] Amorphous ZIF-8 colloidal dispersion was analogously prepared by the reaction of $Zn(CH_3COO)_2{\cdot}2H_2O$ and Hmim in methanol at room temperature (Supporting Information, Figures S22, S23A). A slight sediment occurs probably owing to the fast interaction between Zn^{II} and Hmim ligands, which can be readily filtered out. High-quality films of ZIF-8 were then made by spray coating ZIF-8 colloidal solution onto FTO glass substrate, showing exceptional mechanical robustness (Supporting Information, Figure S23B–D).

Conclusion

Our results demonstrate an inexpensive and convenient spray-coating route to thin, compact and uniform MOF films up to tens of centimeters length scale that were previously unattainable. The spray-coated MOF thin films rely on the unprecedented well-dispersed colloidal dispersions consisting of amorphous MOF nanoparticles, which we used as precursors that readily converted to the crystalline films upon in situ heating. The "sticky" precursor colloidal solution can be deposited onto a number of substrates such as FTO, glass, SiO_2, Al_2O_3, Si, Cu, and even flexible polycarbonate, compatible with future application of MOF thin films in varies technological areas where specific substrate is essential. Although we have focused on the fabrication of uniform ZIF-67 and ZIF-8 films, our present results mark a great promise in producing other high-quality MOF thin films on a large scale.

Acknowledgements

We acknowledge the funding support from the National Natural Science Foundation of China (Grants U1932213, 21431006, 21761132008, 21975237, 51702312), the Foundation

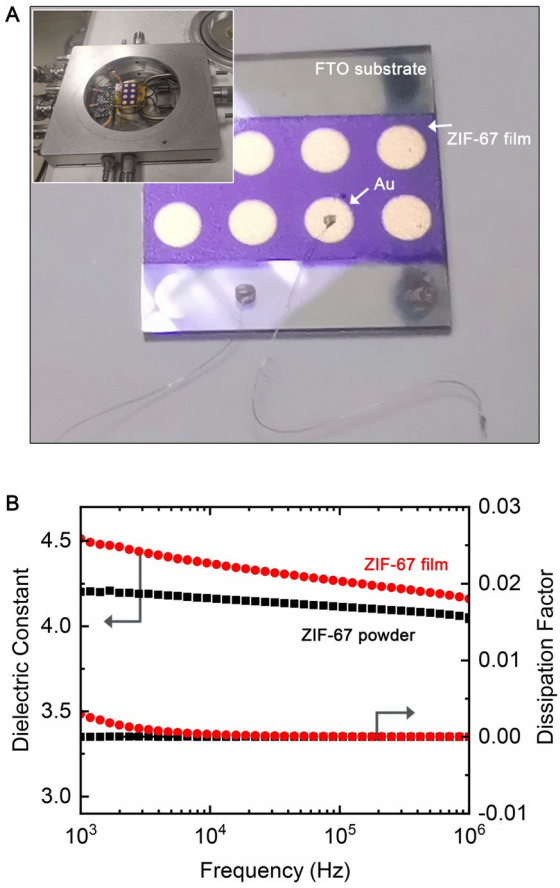

Figure 4. A) Photograph of the device made by ZIF-67 film sputtered with gold for dielectric measurements. Inset photograph: film testing in the chamber. B) Dielectric constant *k* and dissipation factor of ZIF-67 film and ZIF-67 powder.

for Innovative Research Groups of the National Natural Science Foundation of China (Grant 21521001), the National Basic Research Proram of China (Grant 2018YFA0702001), the Users with Excellence and Scientific Research Grant of Hefei Science Center of CAS (2015HSC-UE007), the Strategic Priority Research Program of the Chinese Academy of Sciences (XDA21000000), and the Recruitment Program of Global Youth Experts.

Conflict of interest

The authors declare no conflict of interest.

Keywords: crystallization · metal–organic frameworks · thin films · ZIF-67

[1] H. Furukawa, N. Ko, Y. B. Go, N. Aratani, S. B. Choi, E. Choi, A. O. Yazaydin, R. Q. Snurr, M. O'Keeffe, J. Kim, O. M. Yaghi, *Science* **2010**, *329*, 424–428.
[2] O. M. Yaghi, M. O'Keeffe, N. W. Ockwig, H. K. Chae, M. Eddaoudi, J. Kim, *Nature* **2003**, *423*, 705–714.
[3] H. Furukawa, K. E. Cordova, M. O'Keeffe, O. M. Yaghi, *Science* **2013**, *341*, 1230444.
[4] a) S. Zhou, Y. Wei, L. Li, Y. Duan, Q. Hou, L. Zhang, L. X. Ding, J. Xue, H. Wang, J. Caro, *Sci. Adv.* **2018**, *4*, eaau1393; b) A. Cadiau, K. Adil, P. M. Bhatt, Y. Belmabkhout, M. Eddaoudi, *Science* **2016**, *353*, 137–140; c) X. Cui, K. Chen, H. Xing, Q. Yang, R. Krishna, Z. Bao, H. Wu, W. Zhou, X. Dong, Y. Han, B. Li, Q. Ren, M. J. Zaworotko, B. Chen, *Science* **2016**, *353*, 141–144; d) A. Knebel, B. Geppert, K. Volgmann, D. I. Kolokolov, A. G. Stepanov, J. Twiefel, P. Heitjans, D. Volkmer, J. Caro, *Science* **2017**, *358*, 347–351; e) L. Li, R. B. Lin, R. Krishna, H. Li, S. Xiang, H. Wu, J. Li, W. Zhou, B. Chen, *Science* **2018**, *362*, 443–446; f) P. Q. Liao, N. Y. Huang, W. X. Zhang, J. P. Zhang, X. M. Chen, *Science* **2017**, *356*, 1193–1196.
[5] a) M. P. Suh, H. J. Park, T. K. Prasad, D. W. Lim, *Chem. Rev.* **2012**, *112*, 782–835; b) Y. Peng, V. Krungleviciute, I. Eryazici, J. T. Hupp, O. K. Farha, T. Yildirim, *J. Am. Chem. Soc.* **2013**, *135*, 11887–11894; c) R. Banerjee, A. Phan, B. Wang, C. Knobler, H. Furukawa, M. O'Keeffe, O. M. Yaghi, *Science* **2008**, *319*, 939–943; d) M. Eddaoudi, J. Kim, N. Rosi, D. Vodak, J. Wachter, M. O'Keeffe, O. M. Yaghi, *Science* **2002**, *295*, 469–472.
[6] a) M. S. Yao, X. J. Lv, Z. H. Fu, W. H. Li, W. H. Deng, G. D. Wu, G. Xu, *Angew. Chem. Int. Ed.* **2017**, *56*, 16510–16514; *Angew. Chem.* **2017**, *129*, 16737–16741; b) G. Lu, J. T. Hupp, *J. Am. Chem. Soc.* **2010**, *132*, 7832–7833; c) J. Dong, K. Zhang, X. Li, Y. Qian, H. Zhu, D. Yuan, Q. H. Xu, J. Jiang, D. Zhao, *Nat. Commun.* **2017**, *8*, 1142.
[7] a) Y. Liu, H. Wang, W. Shi, W. Zhang, J. Yu, B. K. Chandran, C. Cui, B. Zhu, Z. Liu, B. Li, C. Xu, Z. Xu, S. Li, W. Huang, F. Huo, X. Chen, *Angew. Chem. Int. Ed.* **2016**, *55*, 8884–8888; *Angew. Chem.* **2016**, *128*, 9030–9034; b) S. M. Yoon, S. C. Warren, B. A. Grzybowski, *Angew. Chem. Int. Ed.* **2014**, *53*, 4437–4441; *Angew. Chem.* **2014**, *126*, 4526–4530; c) L. Pan, G. Liu, H. Li, S. Meng, L. Han, J. Shang, B. Chen, A. E. Platero-Prats, W. Lu, X. Zou, R. W. Li, *J. Am. Chem. Soc.* **2014**, *136*, 17477–17483; d) S. Sakaida, K. Otsubo, O. Sakata, C. Song, A. Fujiwara, M. Takata, H. Kitagawa, *Nat. Chem.* **2016**, *8*, 377–383; e) Y. Zhong, B. Cheng, C. Park, A. Ray, S. Brown, F. Mujid, J.-U. Lee, H. Zhou, J. Suh, K.-H. J. S. Lee, *Science* **2019**, *366*, 1379–1384.
[8] a) J. D. Xiao, H. L. Jiang, *Acc. Chem. Res.* **2019**, *52*, 356–366; b) J. Lee, O. K. Farha, J. Roberts, K. A. Scheidt, S. T. Nguyen, J. T. Hupp, *Chem. Soc. Rev.* **2009**, *38*, 1450–1459; c) C. M. McGuirk, M. J. Katz, C. L. Stern, A. A. Sarjeant, J. T. Hupp, O. K. Farha, C. A. Mirkin, *J. Am. Chem. Soc.* **2015**, *137*, 919–925; d) W. Zhang, Z. Y. Wu, H. L. Jiang, S. H. Yu, *J. Am. Chem. Soc.* **2014**, *136*, 14385–14388; e) G. Lu, S. Li, Z. Guo, O. K. Farha, B. G. Hauser, X. Qi, Y. Wang, X. Wang, S. Han, X. Liu, J. S. DuChene, H. Zhang, Q. Zhang, X. Chen, J. Ma, S. C. Loo, W. D. Wei, Y. Yang, J. T. Hupp, F. Huo, *Nat. Chem.* **2012**, *4*, 310–316; f) J. S. Seo, D. Whang, H. Lee, S. I. Jun, J. Oh, Y. J. Jeon, K. Kim, *Nature* **2000**, *404*, 982–986; g) H. B. Wu, X. W. D. Lou, *Sci. Adv.* **2017**, *3*, eaap9252.
[9] S. Hermes, F. Schroder, R. Chelmowski, C. Woll, R. A. Fischer, *J. Am. Chem. Soc.* **2005**, *127*, 13744–13745.
[10] a) T. Rodenas, I. Luz, G. Prieto, B. Seoane, H. Miro, A. Corma, F. Kapteijn, I. X. F. X. Llabres, J. Gascon, *Nat. Mater.* **2015**, *14*, 48–55; b) B. Ghalei, K. Sakurai, Y. Kinoshita, K. Wakimoto, A. P. Isfahani, Q. Song, K. Doitomi, S. Furukawa, H. Hirao, H. Kusuda, *Nat. Energy* **2017**, *2*, 17086.
[11] P. C. Lemaire, J. Zhao, P. S. Williams, H. J. Walls, S. D. Shepherd, M. D. Losego, G. W. Peterson, G. N. Parsons, *ACS Appl. Mater. Interfaces* **2016**, *8*, 9514–9522.
[12] a) C. R. Wade, M. Li, M. Dinca, *Angew. Chem. Int. Ed.* **2013**, *52*, 13377–13381; *Angew. Chem.* **2013**, *125*, 13619–13623; b) M. Li, M. Dinca, *J. Am. Chem. Soc.* **2011**, *133*, 12926–12929.
[13] P. Falcaro, K. Okada, T. Hara, K. Ikigaki, Y. Tokudome, A. W. Thornton, A. J. Hill, T. Williams, C. Doonan, M. Takahashi, *Nat. Mater.* **2017**, *16*, 342–348.

[14] I. Stassen, M. Styles, G. Grenci, H. V. Gorp, W. Vanderlinden, S. D. Feyter, P. Falcaro, D. D. Vos, P. Vereecken, R. Ameloot, *Nat. Mater.* **2016**, *15*, 304 – 310.
[15] E. Virmani, J. M. Rotter, A. Mahringer, T. von Zons, A. Godt, T. Bein, S. Wuttke, D. D. Medina, *J. Am. Chem. Soc.* **2018**, *140*, 4812 – 4819.
[16] M. Eddaoudi, D. F. Sava, J. F. Eubank, K. Adil, V. Guillerm, *Chem. Soc. Rev.* **2015**, *44*, 228 – 249.
[17] K. Zhou, B. Mousavi, Z. X. Luo, S. Phatanasri, S. Chaemchuen, F. Verpoort, *J. Mater. Chem. A* **2017**, *5*, 952 – 957.
[18] K. S. Park, Z. Ni, A. P. Cote, J. Y. Choi, R. Huang, F. J. Uribe-Romo, H. K. Chae, M. O'Keeffe, O. M. Yaghi, *Proc. Natl. Acad. Sci. USA* **2006**, *103*, 10186 – 10191.
[19] A. Phan, C. J. Doonan, F. J. Uribe-Romo, C. B. Knobler, M. O'Keeffe, O. M. Yaghi, *Acc. Chem. Res.* **2010**, *43*, 58 – 67.
[20] Y. Zhu, J. Ciston, B. Zheng, X. Miao, C. Czarnik, Y. Pan, R. Sougrat, Z. Lai, C. E. Hsiung, K. Yao, I. Pinnau, M. Pan, Y. Han, *Nat. Mater.* **2017**, *16*, 532 – 536.
[21] a) B. Hachuła, M. Nowak, J. Kusz, *J. Chem. Crystallogr.* **2010**, *40*, 201 – 206; b) H. T. Kwon, H. K. Jeong, A. S. Lee, H. S. An, J. S. Lee, *J. Am. Chem. Soc.* **2015**, *137*, 12304 – 12311; c) Y. Hu, H. Kazemian, S. Rohani, Y. Huang, Y. Song, *Chem. Commun.* **2011**, *47*, 12694 – 12696.
[22] a) Z. Öztürk, M. Filez, B. M. Weckhuysen, *Chem. Eur. J.* **2017**, *23*, 10915 – 10924; b) A. Qiao, T. D. Bennett, H. Tao, A. Krajnc, G. Mali, C. M. Doherty, A. W. Thornton, J. C. Mauro, G. N. Greaves, Y. Yue, *Sci. Adv.* **2018**, *4*, eaao6827.
[23] X. L. Ma, P. Kumar, N. Mittal, A. Khlyustova, P. Daoutidis, K. A. Mkhoyan, M. Tsapatsis, *Science* **2018**, *361*, 1008 – 1011.
[24] a) W. J. Li, J. Liu, Z. H. Sun, T. F. Liu, J. Lu, S. Y. Gao, C. He, R. Cao, J. H. Luo, *Nat. Commun.* **2016**, *7*, 11830; b) Z. G. Gu, S. C. Chen, W. Q. Fu, Q. Zheng, J. Zhang, *ACS Appl. Mater. Interfaces* **2017**, *9*, 7259 – 7264; c) Y. G. Ha, K. Everaerts, M. C. Hersam, T. J. Marks, *Acc. Chem. Res.* **2014**, *47*, 1019 – 1028.
[25] R. Lo Nigro, R. G. Toro, G. Malandrino, V. Raineri, I. L. Fragalà, *Adv. Mater.* **2003**, *15*, 1071 – 1075.
[26] a) R. Warmbier, A. Quandt, G. Seifert, *J. Phys. Chem. C* **2014**, *118*, 11799 – 11805; b) E. Redel, Z. Wang, S. Walheim, J. Liu, H. Gliemann, C. Wöll, *Appl. Phys. Lett.* **2013**, *103*, 091903.
[27] X.-C. Huang, Y.-Y. Lin, J.-P. Zhang, X.-M. Chen, *Angew. Chem. Int. Ed.* **2006**, *45*, 1557 – 1559; *Angew. Chem.* **2006**, *118*, 1587 – 1589.

Manuscript received: March 29, 2021
Accepted manuscript online: April 15, 2021
Version of record online: May 14, 2021

